Aliasing of High-Frequency Sea Surface Height Signals in Swath Satellite Altimetry
Ji Ye

Abstract

Satellite altimeters measure global sea surface height (SSH); a variable crucial to understanding phenomena ranging from high-frequency tides to low-frequency ocean circulation. However, motions that have frequencies that are higher than the altimeter sampling frequency will be aliased into lower frequencies. This study quantifies how the future NASA Surface Water and Ocean Topography (SWOT) swath satellite altimeter mission will alias high-frequency motions in the Gulf Stream region using the SWOT Simulator for Ocean Science. The ocean simulator samples hourly output of the HYbrid Coordinate Ocean Model (HYCOM) along altimeter tracks at a 1-day sampling period (SWOT Fast-sampling orbit), a 10-day sampling period (orbit of Jason, the present-generation nadir altimeter), and a 21-day sampling period (SWOT Science orbit). The Ocean Simulator also adds estimates of instrument noise to the simulated signals. SSH wavenumber spectral density was averaged over tracks in the Gulf Stream region to produce an average spectral density per orbit from hourly sampled HYCOM output representative of a non-aliased SSH signal. The SSH wavenumber spectral density for each orbit lies near $k^{-11/3}$, consistent with surface quasigeostropic (SQG) flow theory. The spectral density computed from the 1-day sampling period most closely resembles the spectral density of the hourly sampled signal. The 10- and 21-day sampling periods introduce aliasing of high-frequency signals, but strong mesoscale signal in the Gulf Stream may overpower the aliased high-frequency signals in SWOT data.

1. Introduction

Satellite altimeters remotely monitor sea surface height (SSH) in the global oceans. Altimeters, such as the current Jason-3 nadir altimeter and the forthcoming Surface Water and Ocean Topography (SWOT) swath altimeter, measure SSH by transmitting microwave radiation to the sea surface [*Fu and Cazenave, 2001*]. The emitted microwaves reflect back to the altimeter after they encounter the sea surface. The Jason altimeter uses the round-trip travel time of the radiated signal to determine the elevation of the sea surface along one-dimensional tracks; SWOT will use a more sophisticated algorithm, involving interferometry, to determine SSH in two-dimensional swaths. SWOT is targeted to launch in 2021, and will carry KA-band Radar Interferometers (KaRIn) that produce SSH measurements over two 50-kilometer swaths and a dual-frequency nadir altimeter that uses single track technology [*Fu et al*., 2012]. In the first 90 days of the SWOT mission, the satellite will use a Fast-sampling orbit in which a single swath is measured once daily. Afterwards, SWOT will change to the Science orbit with a 21-day repeat period for three years. The Science orbit will provide more continuous global coverage whereas the Fast-sampling orbit will provide sparse spatial coverage, since short sampling periods sacrifice spatial coverage. High-frequency signals will be aliased during both the Fast and Science Orbit phases of the mission, especially during the Science Orbit with its longer sampling times. High-frequency signals are also aliased in the present Jason altimeters which sample the ocean with a 10-day repeat period.

The SWOT Simulator for Ocean Science [*Gautier et al*., 2017] quantifies the SWOT altimeter performance in the real ocean by simulating orbits on ocean general circulation models

(OGCMs). SSH from any OGCM is used as an input parameter for the simulator, which then interpolates the hourly sampled OGCM onto altimeter tracks from a given orbit and adds altimeter error and noise according to known technical characteristics of the satellite. The software does not interpolate over time. This means that data is presented for each pass and contains only the SSH at a given time, as in the output of the future SWOT mission. Swaths from the simulator are 120 km wide and will measure SSH in 1 km^2 pixels. A full description of the simulator can be found in *Gautier et al.* [2017]. Simulations investigating swath sampling in OGCMs may help to characterize the effects of aliasing on swath altimetry technology prior to the study of the real ocean where the dynamics remain largely unknown.

Wavenumber spectral density analysis is a common method for describing SSH and identifying signals that contribute to SSH. For instance, *Ray and Zaron* [*2016*] identify internal tides from SSH signals in wavenumber *(k)* spectral density. Interpretation of the wavenumber spectral density of low-frequency signals is often done in light of theories of geostrophic turbulence [*Fu and Cazenave,* 2001]. Dimensional arguments for interior quasigeostrophic (QG) dynamics predict kinetic energy to have a slope of k^{-3} [*Vallis,* 2006], and hence a SSH spectral density to have a slope of k^{-5}. Surface quasigeostrophic flow [SQG; *Blumen et al.*, 1978; *Held et al.,* 1995] has a kinetic energy slope of $k^{-5/3}$, as in 3-dimensional turbulence [*Grant et al.,* 1961], and hence a SSH spectral density with a slope of $k^{-11/3}$. For detailed discussions of and dimensional arguments for interior QG theory see *Vallis,* [2006]. See *Blumen* [1978] and *Held et al.,* [1995] for discussions of SQG theory. Numerous studies using altimeter and/or modeled SSH data have found that regions with strong mesoscale eddies have characteristic wavenumber

spectral densities close to either interior QG or SQG theory [*Stammer* 1997; *Le Traon et al.*, 2008; *Richman et al.*, 2012].

We seek to understand the SSH wavenumber spectra and the impact of aliasing of high-frequency motions in the Gulf Stream region where the SSH signal is heavily influenced by mesoscale eddies shed from western boundary currents [*Le Traon et al*., 2008; *Richman et al*., 2012]. Mesoscale eddies have length scales of tens to hundreds of km and time scales of tens to hundreds of days [*Chelton et al.,* 2007]. Because mesoscale eddies are the primary driver of motion in the Gulf Stream region, SSH wavenumber spectral densities from the region are generally expected to follow interior QG or SQG theory with spectral slopes varying as k^{-5} *or* $k^{-11/3}$ [*Stammer* 1997*; Le Traon et al.,* 2008].

Aliasing of high-frequency motions in altimeters can generate spectral slopes that differ from those predicted by SQG and interior QG theory [*Richman et al., 2012*]. This can cause altimeter measurements to be a misrepresentation of low-frequency ocean dynamics. As a rule, signals with frequencies higher than half the sampling frequency, known as the Nyquist frequency, are aliased into low frequency signals causing corruption of the low-frequency signal [*Parke et al.*, 1987; *Ray et al*., 1998; *Richman et al*., 2012; *Shriver et al*., 2012]. The aliased frequencies of periodic motions are easily calculated and are a function of the frequency of oscillation, the sampling frequency, and the length of the record [*Schlax and Chelton,* 1994]. In regions such as the Gulf Stream where mesoscale eddies are strong, the low-frequency aliased signals may not dominate the altimeter data as heavily as in regions dominated by high-frequency motions such as tides or internal gravity waves. Understanding how aliasing can affect

the slope of wavenumber spectral density in regions governed by different dynamics could lead to more informed interpretations of altimeter data.

Simulations of the HYbrid Coordinate Ocean Model (HYCOM) with 1/25° horizontal resolution were sampled in the Gulf Stream at 1-day, 10-day, and 21-day repeat sampling periods using the SWOT Simulator for Ocean Sciences. The HYCOM simulations used in this study, described in detail in Section 2.1, are forced by both atmospheric fields and the astronomical tidal potential. Therefore, they contain both mesoscale eddies and higher-frequency motions such as tides [*Arbic et al*., 2004] and internal gravity waves [*Muller et al.*, 2015]. The 1- and 21-day sampling periods were chosen to represent SWOT's Fast-sampling and Science orbits, respectively. The 10-day period reflects the sampling period of the current day Jason satellite altimeter. The main objectives of this study are (1) to compare changes in SSH spectral density computed from hourly sampled HYCOM to spectral density computed from output subsampled at three different sampling frequencies corresponding to the SWOT Fast-sampling orbit, the Jason orbit, and the SWOT Science orbit; and (2) to discuss the effect of aliasing of high-frequency motions. The Gulf Stream region is selected as an example of a region with strong mesoscale eddy activity; future extensions of this study will consider other important regions in the world ocean. The effect of aliasing in the Gulf Stream region is revealed by the differences in the slopes of SSH wavenumber spectral density computed over the region and along a single altimeter track between the three orbits and hourly sampled HYCOM. The SWOT Ocean Simulator is also capable of simulating the impact of instrumental noise on SSH wavenumber spectral density. Our results may provide insight into how wavenumber spectral densities could

appear in SWOT sampling of the Gulf Stream, and may therefore be useful in planning for SWOT and future satellite altimeter missions.

2. Methods

2.1 The HYCOM Simulation

The HYCOM simulation used in this study is a global simulation with 1/25° horizontal resolution at the equator (approximately 3.5 km) and 41 hybrid layers in the vertical direction. HYCOM is forced by the astronomical tidal potential [*Cartwright*, 1999] of the five largest semidiurnal and diurnal (M_2, S_2, N_2, K_1 and O_1). To minimize the large-scale (barotropic) sea surface elevation errors of M_2, the largest tidal constituent, an Augmented State Ensemble Kalman filter [*Ngodock et al.,* 2016] was employed. The parameterized topographic internal wave drag [*Jayne and St. Laurent*, 2001] used in this simulation was tuned for a prior, lower horizontal (1/12.5º) resolution barotropic tidal simulation [*Buijsman et al.,* 2015], and was not retuned due to high computational cost. HYCOM is forced every three hours by the US Navy Global Environmental Model (NAVGEM) to incorporate atmospheric pressure, wind, and buoyancy forces [*Hogan et al.,* 2014]. A detailed explanation of the model and the differences between the modeled SSH and SSH measured in tide gauges can be found in *Savage et al.,* [2017].

The Gulf Stream region is defined here as ranging in latitude from 22.00º N to 41.79º N and longitude from 38.36°W to 62.64°W as shown in Figure 1. One year of hourly HYCOM SSH, spanning in time from January to December 2014 and taken from the Gulf Stream region, was used as input for the simulator. The simulator interpolates model output to tracks, and

provides along-track SSH measurements both with and without estimates of instrument noise [*Gaultier et al*., 2016, 2017]. Three orbits were chosen to compare SSH signal aliasing. The 1-day SWOT Fast-sampling orbit sampled the Gulf Stream regions along two tracks, while the 10-day Jason orbit, and the 21-day SWOT Science orbits sampled along 20 and 41 tracks, respectively. The number of altimeter tracks in each orbit reflects the tradeoff between altimeter coverage, or the distance between tracks, and the sampling frequency of a given track. Therefore, frequent sampling reduces the number of tracks captured, and less frequent sampling increases the number of tracks captured. In the simulator, the Jason orbit mimics the current Jason altimeter in track location and sampling period only. The tracks in the Jason orbit are the swath tracks of the SWOT altimeter, as opposed to the one-dimensional tracks of current day altimeter technology.

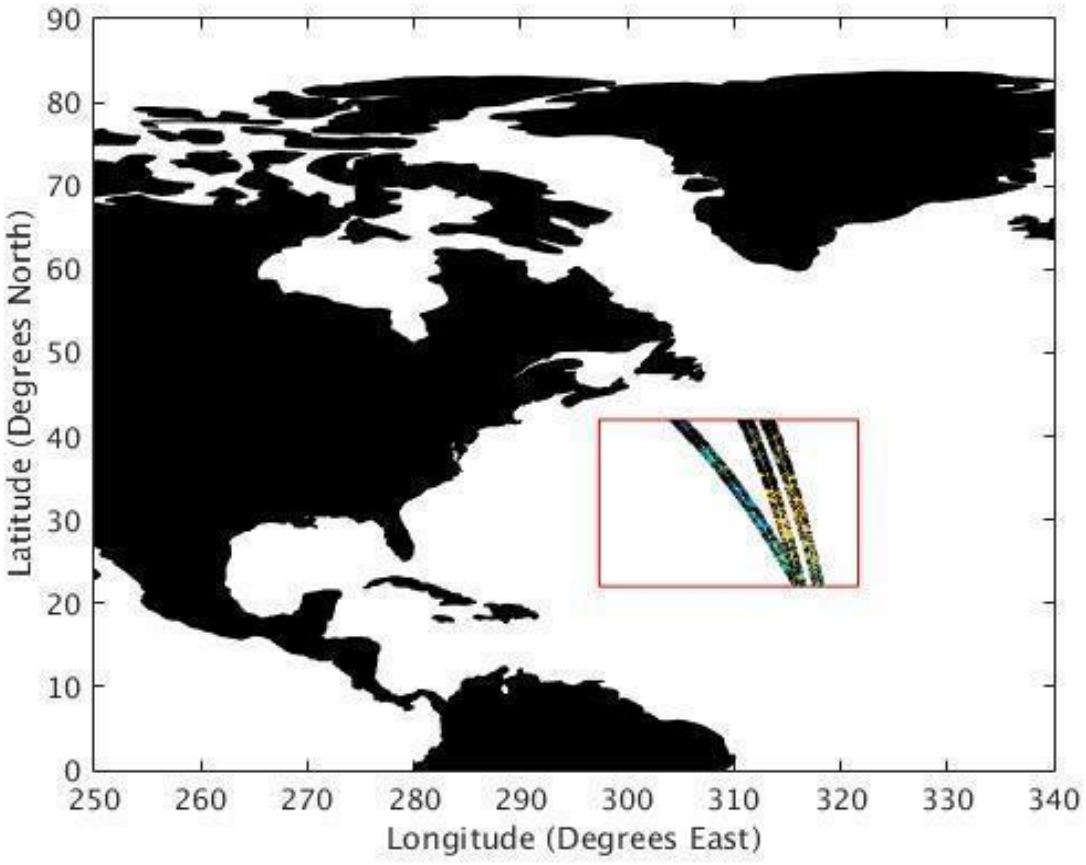

Figure 1. The region used as input for the SWOT Ocean Simulator, ranging in latitude from 22.00°N to 41.79°N and longitude from 38.36°W to 62.64°W. This is a region of strong mesoscale eddies associated with the Gulf Stream, a large western boundary current. From left to right, the three representative tracks within the region correspond to tracks from Jason, the SWOT Science orbit, and the SWOT Fast-sampling orbit, respectively. These tracks were chosen based on similar track length and spatial proximity to each other.

2.2 Wavenumber Spectral Density Calculations

To compute SSH wavenumber spectral density for each track from SWOT Simulator for Ocean Science, a discrete Fourier transform was performed given by

$$\widehat{SSH}(k) = \sum_{t=0}^{X-1} SSH(x)e^{-2\pi k/\mathrm{X}} \qquad (1)$$

where *k* is wavenumber (*1/wavelength*), *x* is time, and X is the total number of samples. Each swath snapshot taken by the simulator is saved as a pass, and sampling period determines the number of passes for each track. SSH varies over a large range of spatial scales and can be represented as a superposition of waves of different wavelengths. The Fourier transform $\widehat{SSH}(k)$ determines the amplitude of the signal as a function of wavelength, which is then represented as a Fourier coefficient, in the wavenumber domain.

This is then translated into a spectral density equal to a normalized square of the Fourier coefficients given by

$$\text{Wavenumber spectral density} = \frac{2\delta x}{X}\left|\widehat{SSH}(k)\right|^2 \qquad (2)$$

The slope of the SSH wavenumber spectral density can be used to determine the dominant dynamics of a region, as described in the introduction.

To understand how well each orbit captures the dynamics of a region, we produced an average wavenumber spectral density over the entirety of the Gulf Stream region shown in Figure 1, and the representative tracks are used in an analysis described later. The wavenumber spectral densities computed along every track in each of the three orbits were interpolated to the length of the spectral density computed from the longest track in its orbit. After interpolation, all tracks within an orbit were averaged together into one spectral density that represented the orbit within the Gulf Stream region.

To identify differences between the three sampling frequencies more clearly, we

computed a time averaged wavenumber spectral density from a representative track in each orbit (Figure 1). The hourly HYCOM SSH output is also interpolated to the track from each orbit, and along track spectral densities are computed for every hourly sample and averaged in time. The latter estimate is taken as "model truth"; i.e. the spectra computed from output that is frequently sampled in time and free of instrumental error. This procedure permits comparison between the average spectral density from the subsampled altimeter data with model truth, the average spectral density computed from hourly samples of the same tracks. In this way, we can understand how the temporal subsampling and instrumental noise impact the wavenumber spectral densities estimated from present-generation nadir- and future-generation swath-altimeters.

3. Results

Horizontal wavenumber spectral densities from the regionally averaged SWOT Fast-sampling, Jason, and SWOT Science orbits are shown in Figure 2. The spectral densities closely follow slopes associated with interior SQG ($k^{-11/3}$) and QG (k^{-5}) theory. However, there is a clear difference in the location of peaks and slopes between spectral densities computed from data sampled at different periods. The spectral density computed from the SWOT Science orbit most closely follows a slope of k^{-5} between wavenumbers of 10^{-2} and 10^{-1} cycles per kilometer (cpkm). The SWOT Science orbit appears to produce the steepest slope of the three orbits. Additionally, the SWOT Science orbit most closely follows SQG $k^{-11/3}$ prediction. The slope of wavenumber spectral density of the Jason orbit is similar to that of daily SWOT Fast-sampling orbit. At wavenumbers less than 10^{-1} cpkm, spectral density slopes vary between and around k^{-5} and $k^{-11/3}$.

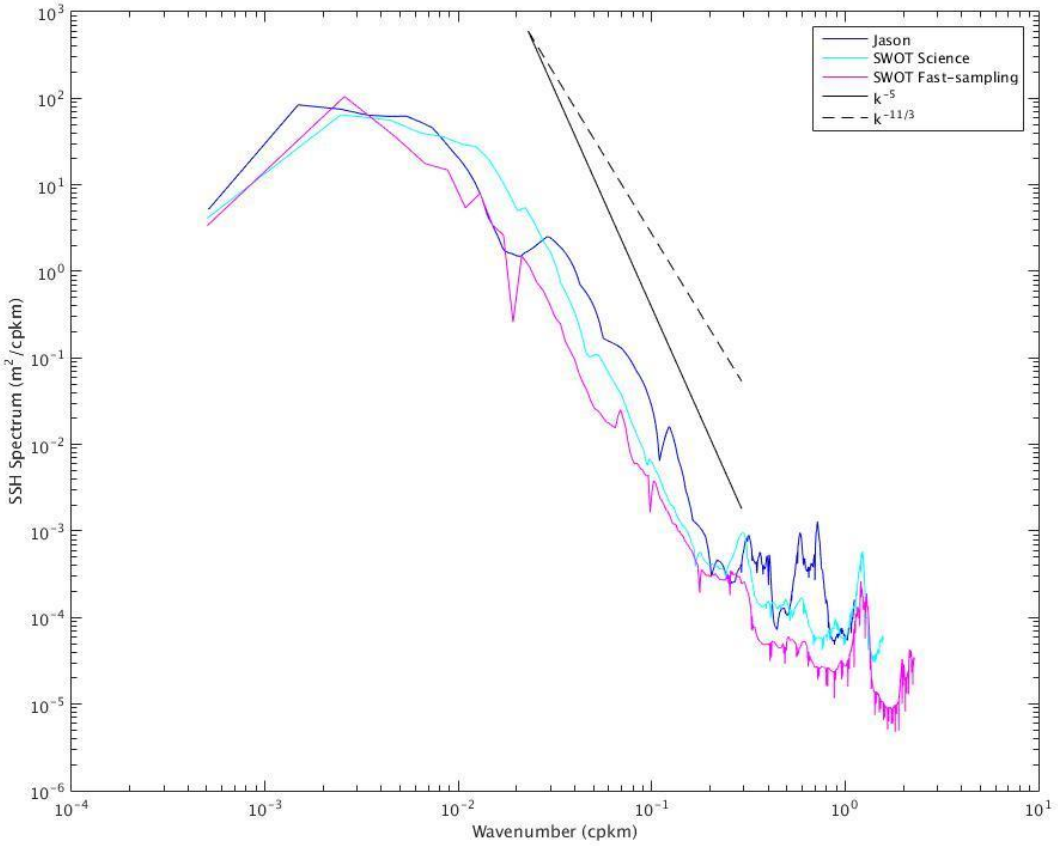

Figure 2. SSH wavenumber spectral density without altimeter noise averaged over all passes and all tracks captured in the Gulf Stream region. Tracks were created by running the SWOT Ocean Simulator over HYCOM output for each orbit to simulate expected SWOT mission tracks. Two SWOT Fast-sampling tracks were averaged together, 41 SWOT Science tracks were averaged together, and 20 Jason tracks were averaged together to produce the blue, cyan, and magenta spectra, respectively.

In the single-track analysis (Figure 3), spectral slopes for all orbits vary closer to $k^{-11/3}$ than to k^{-5} and therefore seem to follow SQG theory rather than interior QG theory. In the SWOT Fast-sampling orbit, all spectral densities are nearly identical with similar slopes and peaks at smaller wavenumbers (Figure 3a). However, the spectral density with altimeter noise flattens out

at wavenumbers greater than 10^{-1} cpkm and has a slope of nearly zero. The slope of the spectral density without altimeter noise is not horizontal at wavenumbers greater than 10^{-1} cpkm but is less steep than at wavenumbers less than 10^{-1} cpkm, implying a deviation from SQG or interior QG theory at wavenumbers greater than 10^{-1} cpkm.

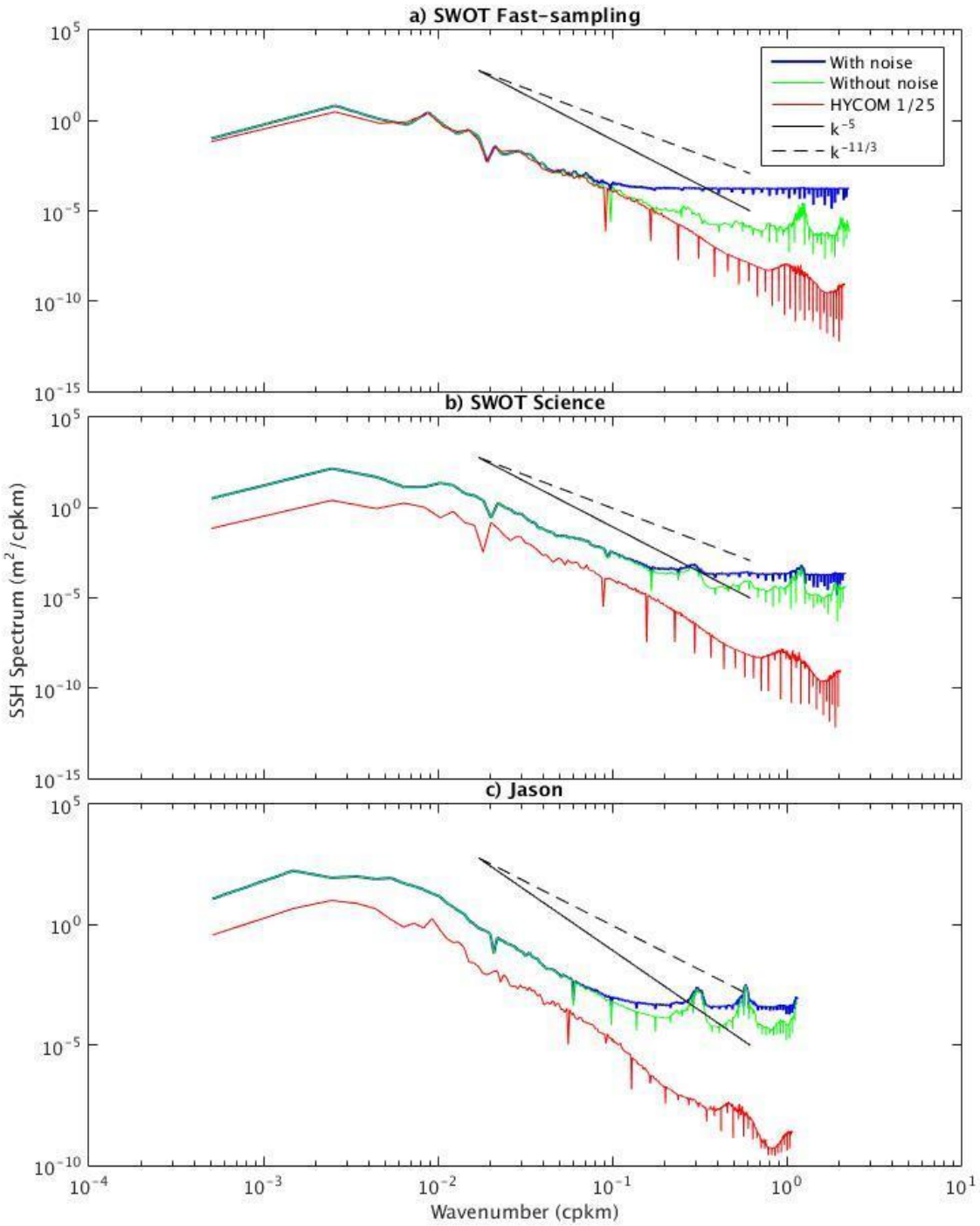

Figure 3. Temporally averaged SSH spectral densities of three tracks within the Gulf Stream region corresponding to (a) SWOT Fast-sampling orbit with repeat period of once per day, and

(b) SWOT Science orbit with repeat period of once per 21 days, and (c) Jason repeat period of once per 10 days. Blue spectral densities contain altimeter noise generated by the SWOT Simulator for Ocean Science. Green spectral densities do not have altimeter noise. The red spectral densities represent hourly sampling of the HYCOM model or the model unaffected by aliasing and instrument error. A line with slope of -5 and -11/3 is plotted against spectral densities from each orbit to show similarities to interior QG theory and SQG theory respectively.

SSH spectral densities of a single track from the Jason and SWOT Science orbits exhibit similar patterns (Figures 3b and 3c). SWOT Science and Jason orbits both yield spectral densities that differ from the hourly sampled tracks (denoted as HYCOM 1/25 in the legend of Figure 3) by a factor of 100. Aside from this, the spectral density computed from the SWOT Science orbit follows nearly the same slope as the spectral density computed from hourly sampled tracks until wavenumbers greater than 10^{-1} cpkm are reached. Spectral densities with altimeter noise from SWOT Science and SWOT Jason orbits flatten out at wavenumbers greater than 10^{-1} cpkm.

Additionally, both SWOT Science and Jason orbit spectral densities contain peaks at wavenumbers that are not indicative of dynamics in the model as they do not appear in the spectral densities computed from the hourly sampled tracks. These are near 9.24×10^{-1} cpkm and 6.05×10^{-1} cpkm in the spectral density of the noise corrected SWOT Science orbit (Figure 3a). The Jason orbit misses many peaks and deviates the most in slope changes from the spectral density computed from hourly sampled tracks (Figure 3c). Obvious deviations are near wavenumbers 10^{-2} cpkm, 2.4×10^{-2} cpkm, and 3.07×10^{-1} cpkm.

4. Discussion

The wavenumber spectral densities computed in the Gulf Stream region follow the SQG theory of spectral density slope varying as $k^{-11/3}$, thus corroborating activity dominated by mesoscale eddies. This result is consistent with previous measurements of spectral slopes in this region [e.g. *Parke et al.,* 1987; *Schlax and Chelton,* 1994; *Ray et al.,* 1998; *Richman et al.,* 2012].

The averaged spectral slope for each of the three orbits over the entire region are not identical (Figure 2). High frequency motions are being aliased in the results. Since mesoscale eddies are low frequency they are not aliased by sampling periods in these altimeter simulations. However, it is possible that the dominance of mesoscale eddies minimizes the amount of aliasing occurring in the Gulf Stream region compared to other regions [*Richman et al.,* 2012].

Differences in SSH wavenumber spectral densities (Figure 2) may partly be a result of the method of averaging spectra over the entire Gulf Stream region. Altimeter tracks varied in length and taking an average over these tracks of different sizes could have led to error. This effect can be minimized by using long tracks that are the same length. Additionally, each orbit sampled from different tracks within the Gulf Stream region; therefore, the orbits did not collect data from the same locations or provide the same coverage. For instance, the SWOT Fast-sampling orbit sampled from two tracks in the Gulf Stream region, whereas the SWOT Science orbit sampled from 41 tracks. The wide difference in spatial coverage between the two orbits may imply that changes in ocean dynamics across the Gulf Stream region itself could cause SSH wavenumber spectral density to vary between orbits. Given these results, averaging spectral

densities of tracks over an entire region may not be an appropriate method of comparison, as different locations in the region can yield different spectral densities.

It is also important to note that altimeter noise may account for some of the differences in average spectral densities between orbits, and the effects of noise are apparent in the single-track analysis seen in Figure 3. *Xu and Fu* [2012] have shown that altimeter noise has a detrimental impact on SSH data, and its removal significantly changes spectral slopes nearly everywhere in the ocean. More specifically, spectral slopes are steeper after removing altimeter noise in oceans poleward of the 20° latitudes [*Xu and Fu*, 2012]. For each orbit, the spectral densities computed from the tracks with noise are nearly identical to those computed without noise until wavenumbers of 10^{-1} cpkm or greater, where the slope of the spectral density computed with noise flatten out (Figure 3).

Analysis of spectral densities from single altimeter tracks shows that there is more aliasing in the Jason orbit's 10-day sampling than in the SWOT science orbit's less frequent sampling (Figures 3b and 3c). This is apparent from increased deviation of the Jason spectral densities from the spectral densities computed using hourly samples compared to those of the SWOT Science orbit. These results are surprising and may be anomalous, since aliasing is thought to be the result of low sampling periods. These observations need to be substantiated with analysis of other tracks within the Gulf Stream region and others to determine whether this is a persistent pattern.

Spectral density slopes of the single tracks appear to be consistent with SQG turbulence theory, though further quantification of slopes is necessary to describe slopes accurately (Figure

3). SSH wavenumber spectral densities calculated from existing altimeter data in the Gulf Stream have previously been examined in several studies indicating SQG dynamics. For instance, *Stammer* [*1997*] obtained a SSH spectrum in the Gulf Stream region to be close to k^{-4} from three years of data from TOPEX/Poseidon. *Le Traon et al*. [2008] found a slope of approximately $k^{-11/3}$ from 15 years of data from TOPEX/Poseidon, Jason-1, Geosat Follow-On, and Envisat and suggested that SQG dynamics play a larger role than interior QG dynamics in the Gulf Stream.

The Gulf Stream region is only one region in the global ocean. Therefore, it would be useful to compare this region against others dominated by different dynamics to better understand the impacts of aliasing. Intense mesoscale eddying from major western boundary currents also characterize the Kuroshio and Agulhas regions [*Le Traon et al.*, 2008]. These regions should therefore be less affected by aliasing of high frequency motions and should yield SSH spectral slopes like that of the Gulf Stream. Conversely, parts of the ocean with strong internal tides and weak mesoscale eddies, such as the North Pacific, should show more aliasing than those with intense mesoscale eddying [*Sasaki and Klein*., 2012; *Richman et al.*, 2012]. Analysis of SSH wavenumber spectral density computed from a region like the Southeast Pacific, which has weak flows in both the low-frequency mesoscale regime and the high-frequency internal gravity wave regime, would provide a contrast to both eddying and internal wave driven regions. The work done here will be expanded upon in summer 2017 to include more regions of the world ocean.

5. Conclusion

SSH wavenumber spectral density in the Gulf Stream region was computed from three satellite altimeter orbits using the SWOT Simulator for Ocean Science in conjunction with a high-horizontal resolution simulation of HYCOM with atmospheric and tidal forcing. Aliasing is exhibited in the 1-day SWOT fast-sampling orbit, 10-day Jason-3 orbit, and a 21-day SWOT science orbit averaged over the entire Gulf Stream region. However, spectral densities computed over a single-track reveal that little-to-no aliasing occurs under the 1-day SWOT Fast-sampling period. Aliasing in the Jason-3 orbit appears greater than that in the SWOT Science orbit, though the SWOT Science orbit does exhibit aliasing, particularly at smaller scales. Wavenumber spectral densities have slopes near those predicted from SQG theory, but a more rigorous approach to quantifying these slopes is necessary as this work is expanded.

One explanation for the differences between the SSH spectral densities averaged over all tracks in the region from the three orbits is the difference in coverage of the Gulf Stream region provided by each orbit. Comparisons of spectral densities computed from a single track in each orbit show that the 1-day SWOT Fast-sampling orbit generates spectral densities that are nearly identical to the spectral density computed from an hourly sampled track and, therefore, appears to limit aliasing. Comparisons of other tracks from the Gulf Stream region using the single-track comparison method can determine if results in this study hold true for other tracks in the region.

Conducting studies with the SWOT Simulator for Ocean Science in different regions with dissimilar dynamics will help clarify the role of temporal aliasing across the global ocean. Studies such as these will inform the community on the effects of aliasing in SWOT data when it

becomes available.

Acknowledgements

I would like to give many thanks to Anna Savage and Brian Arbic for advising me on this project and working with me to realize this thesis. I would also like to thank Joseph Ansong for always having an answer to my Matlab questions. Brian Arbic and I acknowledge support from Research Experience for Undergraduate (REU) supplements to National Science Foundation (NSF) grant number OCE-1351837. Anna Savage acknowledges support from NASA Earth and Space Science Fellowship grant NNX16AO23H. Anna Savage and Brian Arbic were also funded by Office of Naval Research grants N00014-15-1-2288 and N00014-11-1-0487, and NASA grants NNX13AD95Q and NNX16AH79G.

References

Arbic, B. K., S. T. Garner, R. W. Hallberg, and H. L. Simmons (2004), The accuracy of surface elevations in forward global barotropic and baroclinic tide models, *Deep Sea Res.*, Part II, 51, 3069–3101, doi:10.1016/j.dsr2.2004.09.014.

Blumen, W. (1978), Uniform potential vorticity flow: Part I: Theory of wave interactions and two-dimensional turbulence, *J. Atmos. Sci*., 35(5), 774–783, doi:10.1175/1520-0469(1978)035<0774:UPVFPI>2.0.CO;2.

Buijsman, M. C., B. K. Arbic, J. A. M. Green, R. W. Helber, J. G. Richman, J. F. Shriver, P. G. Timko, and A. J. Wallcraft (2015), Optimizing internal wave drag in a forward barotropic model with semidiurnal tides, *Ocean Modelling*, 85, 42–55, doi:10.1016/j.ocemod.2014.11.003.

Cartwright, D. E. (1999), *Tides: A Scientific History*, 192 pp., Cambridge Univ. Press, Cambridge, U. K.

Chelton, D. B., M. G. Schlax, R. M. Samelson, and R. A. de Szoeke (2007), Global observations of large oceanic eddies, *Geophys. Res. Lett*., 34(15), 1944-8007, doi:10.1029/2007GL030812.

Fu, L. L., and A. Cazenave (Eds.) (2001), *Satellite Altimetry and Earth Sciences: A Handbook of Techniques and Applications*, Academic, San Diego, Calif.

Fu, L. L., D. Alsdorf, R. Morrow, E. Rodriguez, and N. Mognard (Eds.) (2012), *SWOT: The Surface Water and Ocean Topography Mission: Wide-Swatch Altimetric Measurement of Water Elevation on Earth*, Jet Propul. Lab., Pasadena, Calif.

Gaultier, L., C. Ubelmann, and L. Fu (2016), The challenge of using future SWOT data for oceanic field reconstruction, *J. Ocean. Atm. Tech.,* 33, 119-126, doi:10.1175/JTECH-D-15-0160.1.

Gaultier, L., C. Ubelmann, and L. Fu (Eds.) (2017), *SWOT Simulator Documentation Release 2.3.0.*

Grant, H.L., R.W. Stewart, and A. Moillet (1961) Turbulence spectra from a tidal channel, *J. Fluid Mechanics*, 12, 241-263, doi:10.1017/S002211206200018X.

Held, M., Pierrehumbert, R., Garner, S., and K. Sawson, (1995), Surface quasigeostrophic dynamics, *Journal of Fluid Dynamics,* 282, 1-20, doi:10.1.1.144.3654.

Hogan, T. F., et al. (2014), The navy global environmental model, *Oceanography*, 27(3), 116–125, doi:10.5670/oceanog.2014.73.

Jayne, S. R., and L. C. St. Laurent (2001), Parameterizing tidal dissipation over rough topography, *Geophys. Res. Lett*., 28, 811–814, doi:10.1029/2000GL012044.

Le Traon, P. Y., P. Klein, B. L. Hua, and G. Dibarboure (2008), Do altimeter wavenumber spectra agree with the interior or surface quasigeostrophic theory*? J. Phys. Oceanogr*., 38(5), 1137-1142, doi:10.1175/2007JPO3806.1

Muller, M., B. K. Arbic, J. G. Richman, J. F. Shriver, E. L. K. R. B. Scott, A. J. Wallcraft, and L. Zamudio (2015), Toward and internal gravity wave spectrum in global ocean models, *Geophys. Res. Lett.*, 42, 3474–3481, doi:10.1002/2015GL063365.

Ngodock, H. E., I. Souopgui, A. J. Wallcraft, J. G. Richman, J. F. Shriver, and B. K. Arbic (2016), On improving the accuracy of the M2 barotropic tides embedded in a high-resolution global ocean circulation model, Ocean Modelling, 97, 16–26, doi: 10.1016/j.ocemod.2015.10.011.

Parke, M., R. Steward, D. Farless, and D. Cartwright (1987), On the choice of orbits for an altimetric satellite to study ocean circulation and tides, *Journal of Geophysical Research-Oceans*, 92(11), 11693-11707, doi: 10.1029/JC092iC11p11693.

Ray, R. D. (1998), Ocean self-attraction and loading in numerical tidal models, *Marine Geodesy*, 21(3), 181–192, doi:1080/01490419809388134.

Ray, R. D., and E. D. Zaron (2016), M_2 internal tides and their observed wavenumber spectra from satellite altimetry, *J. Phys. Oceanogr*., 46, 3–22, doi:10.1175/JPO-D-15-0065.1.

Richman, J. G., B. K. Arbic, J. F. Shriver, E. J. Metzger, and A. J. Wallcraft (2012), Inferring dynamics from the wavenumber spectra of an eddying global ocean model with embedded tides, *Journal of Geophysical Research-Oceans*, 117(12), 2156-2202, doi: 10.1029/2012JC008364.

Sasaki, H. and P. Klein (2012), SSH wavenumber spectra in the north pacific from a high-resolution realistic simulation, *J. Phys. Oceanogr*., 42(7), 1233-1241. doi:10.1175/JPO-D-11-0180.1.

Savage, A. C., B. K. Arbic, J. G. Richman, J. F. Shriver, M. H. Alford, M. C. Buijsman, J. Thomas Farrar, H. Sharma, G. Voet, A. J. Wallcraft, and L. Zamudio (2017), Frequency content of sea surface height variability from internal gravity waves to mesoscale eddies, *Journal of Geophysical Research-Oceans*, 122, doi:10.1002/2016JC012331.

Schlax, M. and D. Chelton (1994), Aliased tidal errors in topex/poseidon sea-surface height data, *Journal of Geophysical Research-Oceans*, 99(12), 24761-2477, doi:10.1029/94JC01925

Shriver, J. F., B. K. Arbic, J. G. Richman, R. D. Ray, E. J. Metzger, A. J. Wallcraft, and P. G. Timko (2012), An evaluation of the barotropic and internal tides in a high-resolution global ocean circulation model, *Journal of Geophysical Research-Oceans*, 117(10), 2156-2202, doi:10.1029/2012JC008170.

Stammer, D. (1997). Global characteristics of ocean variability estimated from regional topex/poseidon altimeter measurements. *J. Phys. Oceanogr.*, 27**,** 1743–1769, doi: 10.1175/1520-0485(1997)027<1743:GCOOVE>2.0.CO;2.

Vallis, G. K., (2006). *Atmospheric and Oceanic Fluid Dynamics*. Cambridge University Press.

Xu, Y. and L. Fu (2012), The effects of altimeter instrument noise on the estimation of the Wavenumber Spectrum of Sea Surface Height, *J. Phys. Oceanogr*., 42(12), 2229-2233, doi: 10.1175/JPO-D-12-0106.1.